

## Setting the scale for the Lüscher-Weisz action

Christof Gattringer, Roland Hoffmann, and Stefan Schaefer  
*Institut für Theoretische Physik, Universität Regensburg, 93040 Regensburg, Germany*  
 (Received 11 January 2002; published 15 April 2002)

We study the quark-antiquark potential of quenched SU(3) lattice gauge theory with the Lüscher-Weisz action. After blocking the gauge fields with the recently proposed hypercubic transformation, we compute the Sommer parameter, extract the lattice spacing  $a$ , and set the scale at six different values of the gauge coupling in a range from  $a=0.084$  fm to 0.136 fm.

DOI: 10.1103/PhysRevD.65.094503

PACS number(s): 11.15.Ha

Recently, a noticeable revival of interest in improved gauge actions took place. It was observed that improved gauge actions make the numerical problems less severe when implementing chiral fermions. The underlying mechanism for numerical improvement is a suppression of ultraviolet fluctuations of the gauge field. An example is the use of the Iwasaki and other improved gauge actions for domain-wall fermions [1]. Also, using the perfect gauge action [2] is an integral part of constructing the fixed-point Dirac operator [3]. Recently, a systematic expansion of a solution of the Ginsparg-Wilson equation [4], the so-called chirally improved fermion, was proposed and implemented [5]. Also, it was found there that using the improved gauge action is numerically advantageous for the Dirac operator. In particular, the Lüscher-Weisz action [6] with coefficients from tadpole improved perturbation theory [7,8] was used. Subsequently, the instanton content of the QCD vacuum was studied for the Lüscher-Weisz action in [9].

In this article, we report on our results for the static potential and the lattice scale for the Lüscher-Weisz action in order to make the use of this action easily accessible to the community. Furthermore, we test the recently proposed method of hypercubic blocking [10] which was found [10,11] to improve the statistical accuracy in the determination of the static potential by an order of magnitude. We analyze quenched ensembles at six different values of the gauge coupling and compute the Sommer parameter [12,13] and the lattice spacing  $a$ . This results in a precise determination of the lattice scale in a range between  $a=0.084$  fm and  $a=0.136$  fm and using a fit to our data even beyond this interval. Together with our results for the secondary couplings  $\beta_2$  and  $\beta_3$ , this article provides all the necessary ingredients for using the Lüscher-Weisz action at typical lattice spacings of state of the art simulations.

In addition to the plaquette term of the Wilson gauge action, the Lüscher-Weisz action includes a sum over all  $2 \times 1$  rectangles and a sum over all parallelograms, i.e., all possible closed loops of length 6 along the edges of all 3-cubes. Explicitly, the action reads

$$S[U] = \beta_1 \sum_{pl} \frac{1}{3} \text{Re Tr}[1 - U_{pl}] + \beta_2 \sum_{rt} \frac{1}{3} \text{Re Tr}[1 - U_{rt}] + \beta_3 \sum_{pg} \frac{1}{3} \text{Re Tr}[1 - U_{pg}], \quad (1)$$

where  $\beta_1$  is the principal parameter while  $\beta_2$  and  $\beta_3$  can be computed [7] from  $\beta_1$  using one-loop perturbation theory and tadpole improvement [8],

$$\beta_2 = -\frac{\beta_1}{20 u_0^2} [1 + 0.4805 \alpha], \quad \beta_3 = -\frac{\beta_1}{u_0^2} 0.03325 \alpha, \quad (2)$$

with

$$u_0 = (\frac{1}{3} \text{Re Tr}\langle U_{pl} \rangle)^{1/4}, \quad \alpha = -\frac{\ln(\frac{1}{3} \text{Re Tr}\langle U_{pl} \rangle)}{3.06839}. \quad (3)$$

The couplings  $\beta_2, \beta_3$  are determined self-consistently from  $u_0$  and  $\alpha$  for a given  $\beta_1$ . In Table I, we list the values of the  $\beta_i$  used for our ensembles and our results for the expectation value of the plaquette  $u_0^4 = \text{Re Tr}\langle U_{pl} \rangle/3$ . The sample size at each value of  $\beta_1$  is 200 configurations on  $16^4$  lattices. The update was done with a combination of Metropolis and over-relaxation sweeps.

Before measuring the potential, we applied the hypercubic blocking transformation proposed in [10]. Hypercubic blocking mixes only gauge links from the hypercubes attached to the target link and has less of an impact on the short-distance properties of the gauge fields than previously used smearing methods. The hypercubic blocking transformation proceeds in three steps [10]:

$$\begin{aligned} \bar{V}_{i,\mu;v\rho} &= \mathcal{P}_{\text{SU}(3)} \left[ (1 - \alpha_3) U_{i,\mu} + \frac{\alpha_3}{2} \sum_{\pm \eta \neq \rho, v, \mu} U_{i,\eta} U_{i+\hat{\eta},\mu} U_{i+\hat{\mu},\eta}^\dagger \right], \\ \tilde{V}_{i,\mu;v} &= \mathcal{P}_{\text{SU}(3)} \left[ (1 - \alpha_2) U_{i,\mu} + \frac{\alpha_2}{4} \sum_{\pm \rho \neq v, \mu} \bar{V}_{i,\rho;v\mu} \bar{V}_{i+\hat{\rho},\mu;v} \bar{V}_{i+\hat{\mu},\rho;v\mu}^\dagger \right], \\ V_{i,\mu} &= \mathcal{P}_{\text{SU}(3)} \left[ (1 - \alpha_1) U_{i,\mu} + \frac{\alpha_1}{6} \sum_{\pm v \neq \mu} \tilde{V}_{i,v;\mu} \tilde{V}_{i+\hat{v},\mu;v} \tilde{V}_{i+\hat{\mu},v;\mu}^\dagger \right]. \end{aligned} \quad (4)$$

TABLE I. Parameters for the Lüscher-Weisz action. We list the values of the  $\beta_i$  and the expectation value of the plaquette  $u_0^4 = \text{Re Tr}\langle U_{pl} \rangle/3$ .

$\beta_1$	8.00	8.10	8.20	8.30	8.45	8.60
$u_0^4$	0.62107(3)	0.62894(3)	0.63599(3)	0.64252(3)	0.65176(3)	0.66018(3)
$\beta_2$	-0.54574	-0.54745	-0.54998	-0.55332	-0.55773	-0.56345
$\beta_3$	-0.05252	-0.05120	-0.05020	-0.04953	-0.04829	-0.04755

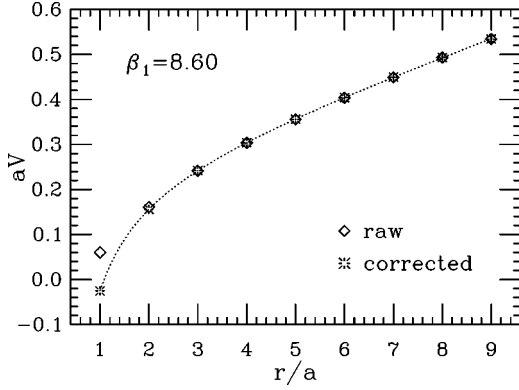


FIG. 1. The static potential for the  $\beta_1=8.60$  ensemble. The diamonds represent the raw data from the two-parameter fit on the Wilson loops and the bursts are the values corrected for the short-distance effect of the hypercubic blocking. The full curve is the parametrization (5).

TABLE II. Results for the Sommer parameter  $r_0$  in lattice units and the corresponding values for the lattice spacing  $a$  when  $r_0$  is assumed as 0.5 fm.

$\beta_1$	8.00	8.10	8.20	8.30	8.45	8.60
$r_0/a$	3.688(37)	4.015(34)	4.362(41)	4.741(49)	5.289(66)	5.967(70)
$a$ (fm)	0.136(1)	0.125(1)	0.115(1)	0.105(1)	0.095(1)	0.084(1)

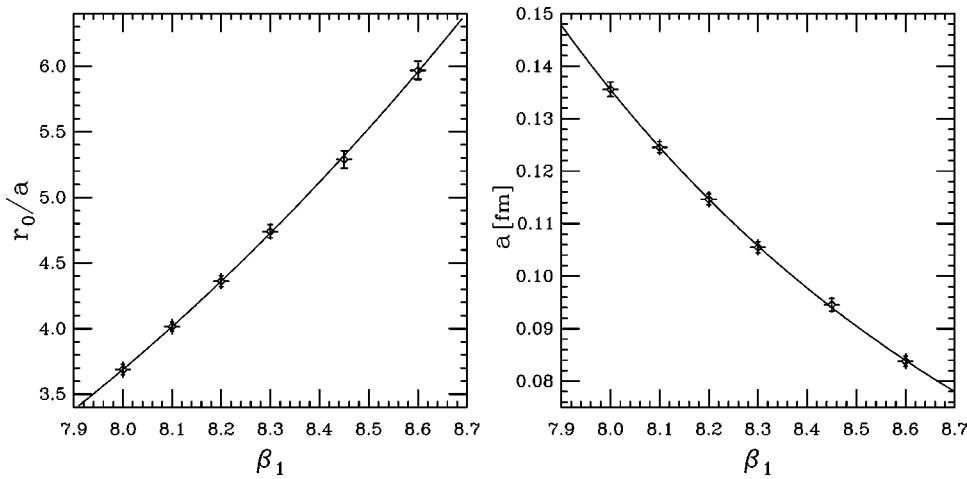


FIG. 2. Results for the Sommer parameter in lattice units (left-hand side) and the lattice spacing in Fermi units (right-hand side) as a function of  $\beta_1$ . The full curves are the interpolations of the data with the function (6).

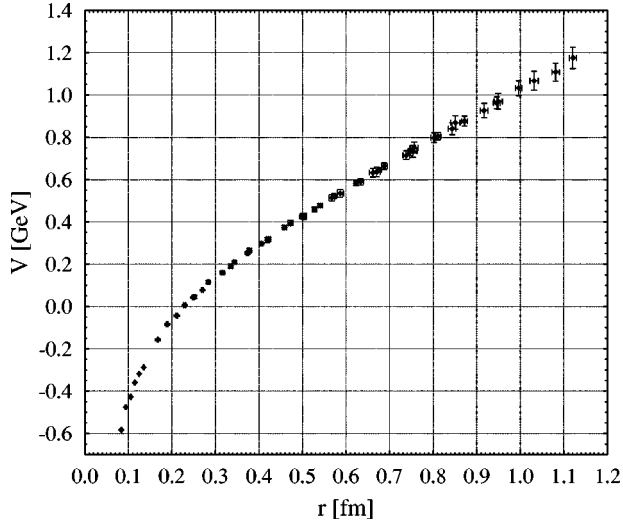


FIG. 3. Superposition of the potentials for all values of  $\beta_1$ . The irrelevant constant  $C$  in formula (5) is set to zero.

In the first step, intermediate fields  $\bar{V}_{i,\mu;\nu\rho}$  are created from the thin-link variables  $U_{i,\mu}$  (indices  $i$  run over all sites of the lattice, and  $\mu, \nu, \rho$ , and  $\eta$  over the four directions). In the second step, the intermediate fields  $\bar{V}_{i,\mu;\nu\rho}$  are blocked into a second set of intermediate fields  $\tilde{V}_{i,\mu;\nu}$  which in the third step are transformed into the final fields  $V_{i,\mu}$ . The restrictions on the indices  $\mu, \nu$ , and  $\rho$  implemented in the sums in Eqs. (4) ensure that  $V_{i,\mu}$  contains only contributions from the hypercubes attached to the link  $(i, \mu)$ . By  $\mathcal{P}_{\text{SU}(3)}$ , we denote the projection of the sums back to elements of  $\text{SU}(3)$ . The parameters  $\alpha_1, \alpha_2$ , and  $\alpha_3$  determine the admixture of staples in each step of the blocking process. These parameters were optimized [10] to minimize the fluctuations of the plaquette. Their values are given by  $\alpha_1=0.75$ ,  $\alpha_2=0.6$ , and  $\alpha_3=0.3$ .

We measured the static potential on the smeared configurations using planar Wilson loops  $W(r, t)$  of size  $r \times t$  with both  $t$  and  $r$  ranging from 1 to 10. We fitted the expectation values of the Wilson loops to a sum of two exponentials  $c_1 \exp(-V(r)t) + c_2 \exp(-E't)$  in a range of  $t=2, 3, \dots, 9$ . The second exponential takes into account the contribution from excited states  $E' > V(r)$ , and from the first term we directly obtain the potential  $V(r)$  for two static sources at distance  $r$ . As a cross check we also computed for some of the ensembles the potential for the raw, unblocked configurations. We find that the results are compatible within error bars but the statistical fluctuations, in particular at larger values of  $r$  and  $t$ , are much more severe for the raw configurations.

In Fig. 1, we show our results for the static potential for the  $\beta_1=8.60$  ensemble. The smooth curve is the standard infrared parametrization for the continuum potential,

$$V(r) = C - A/r + \sigma r, \quad (5)$$

with constants  $C, A$ , and  $\sigma$ . The diamonds are the values for the potential obtained from the Wilson loops. The error bars are smaller than the symbols. For small distances, one finds a noticeable deviation from the Coulomb behavior  $-A/r$ . This deviation is an effect of the hypercubic blocking. However, this effect can be computed perturbatively and the obtained deviation from the Coulomb potential is used to introduce a fourth fit parameter in the potential fit [11]. Subtracting this perturbative part gives the corrected data, which we represent by bursts. From the parameters  $A$  and  $\sigma$ , we computed the Sommer parameter  $r_0$  [13] in lattice units  $a$ , and assuming  $r_0=0.5$  fm we extracted the lattice spacing  $a$ . The result is very stable under variation of the fit range for the potential. Even the  $r/a=1$  measurement can be included. The final result is the weighted average over all fit ranges  $[ar_{\min}, ar_{\max}]$  with  $r_{\min} \in \{1, 2, 3\}$  and  $r_{\max} \in \{7, 8, 9\}$ . We give the results for the lattice spacing and the Sommer parameter in Table II.

Without the improved fit,  $r_0$  can still be determined using Eq. (5). In this case, the lower limit of the fit must be chosen so that the region where the hypercubic smearing distorts the potential is excluded, as can be seen from Fig. 1, i.e.,  $r_{\min} \in \{2, 3\}$ . The results of an analysis based on the three-parameter fit (5) are in perfect agreement with those given in Table II [for, e.g.,  $\beta_1=8.30$  one obtains  $r_0=4.732(43)$ ]. Thus the only benefit from the improved fit is that no data points have to be excluded. This shows that the effect of the hypercubic smearing on the short-distance static quark potential is under good perturbative control.

In order to make the Sommer parameter and the lattice spacing available also for other values of  $\beta_1$ , we fit our data to a functional form based on the  $\beta$  function as proposed in [13]. We find

$$\ln(r_0/a) = 1.553\,54 + 0.798\,40(\beta_1 - 8.3) - 0.095\,33(\beta_1 - 8.3)^2. \quad (6)$$

In Fig. 2, we compare our numerical data for  $r_0/a$  and  $a$  (again assuming  $r_0=0.5$  fm) to the curve (6). It is obvious that the data are well described by our parametrization. Furthermore, when extending the plot range to values of  $\beta_1$  as small as  $\beta_1=6.8$ , we find that our results are in good agreement with the data computed for very coarse lattices in [7], i.e.,  $a=0.24$  fm at  $\beta_1=7.4$ ,  $a=0.33$  fm at  $\beta_1=7.1$ , and  $a=0.40$  fm at  $\beta_1=6.8$ .

Finally, in Fig. 3 we show a common plot of our results for the static potential at all values of  $\beta_1$  we analyzed. We set the irrelevant overall constant  $C$  to zero for all  $\beta_1$ . It is obvious that the data from different lattice spacings are in perfect agreement and the discretization errors are hardly noticeable for the Lüscher-Weisz action.

We would like to thank Meinulf Göckeler, Anna Hasenfratz, Francesco Knechtli, Paul Rakow, and Andreas Schäfer for interesting discussions. C. G. was supported by the Austrian Academy of Sciences (APART 654).

- [1] K. Orginos, Nucl. Phys. B (Proc. Suppl.) **106**, 721 (2002); L.I. Wu, *ibid.* **83**, 224 (2000); A. Ali Khan *et al.*, *ibid.* **83**, 591 (2000).
- [2] T. DeGrand, A. Hasenfratz, P. Hasenfratz, and F. Niedermayer, Nucl. Phys. **B454**, 587 (1995); **B454**, 615 (1995); Phys. Lett. B **365**, 233 (1996).
- [3] P. Hasenfratz, Nucl. Phys. B (Proc. Suppl.) **63**, 53 (1998); Nucl. Phys. **B525**, 401 (1998); P. Hasenfratz, S. Hauswirth, K. Holland, T. Jörg, F. Niedermayer, and U. Wenger, Nucl. Phys. B (Proc. Suppl.) **94**, 627 (2001); P. Hasenfratz, S. Hauswirth, K. Holland, T. Jörg, and F. Niedermayer *ibid.* **106**, 799 (2002).
- [4] P.H. Ginsparg and K.G. Wilson, Phys. Rev. D **25**, 2649 (1982).
- [5] C. Gattringer, Phys. Rev. D **63**, 114501 (2001); C. Gattringer and I. Hip, Phys. Lett. B **480**, 112 (2000); C. Gattringer, I. Hip, and C.B. Lang, Nucl. Phys. **B597**, 451 (2001).
- [6] M. Lüscher and P. Weisz, Commun. Math. Phys. **97**, 59 (1985); **98**, 433(E) (1985); G. Curci, P. Menotti, and G. Paffuti, Phys. Lett. **130B**, 205 (1983); **135B**, 516(E) (1984).
- [7] M. Alford, W. Dimm, G.P. Lepage, G. Hockney, and P.B. Mackenzie, Phys. Lett. B **361**, 87 (1995).
- [8] M. Lüscher and P. Weisz, Phys. Lett. **158B**, 250 (1985); J. Snippe, Nucl. Phys. **B498**, 347 (1997); G.P. Lepage and P.B. Mackenzie, Phys. Rev. D **48**, 2250 (1993).
- [9] C. Gattringer, M. Göckeler, P.E.L. Rakow, S. Schaefer, and A. Schäfer, Nucl. Phys. **B617**, 101 (2001); **B618**, 205 (2001).
- [10] A. Hasenfratz and F. Knechtli, Phys. Rev. D **64**, 034504 (2001).
- [11] A. Hasenfratz, R. Hoffmann, and F. Knechtli, Nucl. Phys. B (Proc. Suppl.) **106**, 418 (2002).
- [12] R. Sommer, Nucl. Phys. **B411**, 839 (1994).
- [13] M. Guagnelli, R. Sommer, and H. Wittig, Nucl. Phys. **B535**, 389 (1998).